PNAS RESEARCH ARTICLE | MICROBIOLOGY OPEN ACCESS

Deletion of a previously uncharacterized lipoprotein lirL confers resistance to an inhibitor of type II signal peptidase in *Acinetobacter baumannii*

Ke-Jung Huang[a], Homer Pantua[a], Jingyu Diao[a], Elizabeth Skippington[b], Michael Volny[c], Wendy Sandoval[c], Varnesh Tiku[a,1], Yutian Peng[a], Meredith Sagolla[d], Donghong Yan[e], Jing Kang[e], Anand Kumar Katakam[d], Nairie Michaelian[f], Mike Reichelt[d], Man-Wah Tan[a], Cary D. Austin[d], Min Xu[e], Emily Hanan[g], and Sharookh B. Kapadia[a,2]

Edited by Jean-Francois Collet, Universite catholique de Louvain, Brussels, Belgium; received December 22, 2021; accepted August 9, 2022 by Editorial Board Member Susan T. Lovett

Acinetobacter baumannii **is a clinically important, predominantly health care–associated gram-negative bacterium with high rates of emerging resistance worldwide. Given the urgent need for novel antibacterial therapies against *A. baumannii*, we focused on inhibiting lipoprotein biosynthesis, a pathway that is essential for envelope biogenesis in gram-negative bacteria. The natural product globomycin, which inhibits the essential type II signal peptidase prolipoprotein signal peptidase (LspA), is ineffective against wild-type *A. baumannii* clinical isolates due to its poor penetration through the outer membrane. Here, we describe a globomycin analog, G5132, that is more potent against wild-type and clinical *A. baumannii* isolates. Mutations leading to G5132 resistance in *A. baumannii* map to the signal peptide of a single hypothetical gene, which we confirm encodes an alanine-rich lipoprotein and have renamed *lirL* (prolipoprotein signal peptidase inhibitor resistance lipoprotein). LirL is a highly abundant lipoprotein primarily localized to the inner membrane. Deletion of *lirL* leads to G5132 resistance, inefficient cell division, increased sensitivity to serum, and attenuated virulence. Signal peptide mutations that confer resistance to G5132 lead to the accumulation of diacylglyceryl-modified LirL prolipoprotein in untreated cells without significant loss in cell viability, suggesting that these mutations overcome a block in lipoprotein biosynthetic flux by decreasing LirL prolipoprotein substrate sensitivity to processing by LspA. This study characterizes a lipoprotein that plays a critical role in resistance to LspA inhibitors and validates lipoprotein biosynthesis as a antibacterial target in *A. baumannii*.**

LspA | *Acinetobacter baumannii* | globomycin | antibiotic resistance

Significance

Inhibiting bacterial lipoprotein biosynthesis in Enterobacteriaceae is an attractive antibacterial strategy to target multidrug resistance, and mechanisms of resistance to prolipoprotein signal peptidase (LspA) inhibitors in *Escherichia coli* are relatively well understood. In contrast, it has been challenging to understand the mechanisms of resistance to LspA inhibitors in *Acinetobacter baumannii* due to the substantially lower inhibitor potencies and the lack of a homologous *lpp* gene. By increasing the antibacterial potency of the LspA inhibitor, globomycin, against wild-type *A. baumannii*, we were able to examine resistance to LspA inhibitors, resulting in the identification of a previously uncharacterized highly abundant lipoprotein, LspA inhibitor resistance lipoprotein. This study reveals insights into resistance mechanisms of *A. baumannii* against inhibitors of bacterial lipoprotein biosynthesis.

Acinetobacter baumannii is a glucose-nonfermentative, nonmotile, aerobic gram-negative coccobacillus and one of the major causes of health care–associated infections, due in part to its antimicrobial resistance capabilities and tolerance to desiccation (1, 2). *A. baumannii* uses multiple mechanisms of resistance to evade antibiotics, including enzymatic degradation of antibiotics, modifications of the antibiotic target, and regulation of multidrug efflux pump expression (2–4). Hospital outbreaks of multidrug-resistant *A. baumannii* infection are increasingly prevalent worldwide (5–7) and according to the World Health Organization, are among the most serious priority 1 threats posed by ESKAPE organisms, which also include *Enterococcus faecium*, *Staphylococcus aureus*, *Klebsiella pneumoniae*, *Pseudomonas aeruginosa*, and *Enterobacter* species. For these reasons, there is an urgent need to identify antibacterials against *A. baumannii* with novel mechanisms of action.

Similar to other gram-negative bacteria, the *A. baumannii* cell envelope consists of a phospholipid inner membrane (IM) and an asymmetrical outer membrane (OM) separated by the periplasm, which contains a peptidoglycan (PGN) cell wall (8). Apart from this overall similarity, there are many differences in the cell wall structure between *A. baumannii* and other gram-negative bacteria, such as *Escherichia coli*. The *A. baumannii* OM contains two types of glycolipids, lipopolysaccharide (LPS) and lipooligosaccharide (LOS) (9), and can uniquely grow in the absence of Lipid A. More recent studies have found increased levels of a number of OM lipoproteins in LOS-deficient *A. baumannii* (10), suggesting that *A. baumannii* can compensate for the lack of LPS by increasing transport of OM lipoproteins. *E. coli* encodes >90 lipoproteins (11, 12), which play essential roles in adhesion, antibiotic resistance, virulence, invasion, and immune evasion (13). Although inhibitors of Lgt and prolipoprotein signal peptidase (LspA) are bactericidal against *E. coli*, these inhibitors lack sufficient potency against nonfermenting bacteria, such as *A. baumannii*. Therefore, we hypothesized that

This article is a PNAS Direct Submission. J.-F.C. is a guest editor invited by the Editorial Board.

[1]Present address: Department of Immuno-Oncology/Functional Genomics, Gilead Sciences, Foster City, CA 94404.

[2]To whom correspondence may be addressed. Email: kapadia.sharookh@gene.com.

This article contains supporting information online at http://www.pnas.org/lookup/suppl/doi:10.1073/pnas.2123117119/-/DCSupplemental.

Published September 13, 2022.

enhancing the antibacterial activity against wild-type *E. coli* may identify analogs with greater antibacterial activity against wild-type *A. baumannii*.

Bacterial lipoprotein biosynthesis is a multistep pathway starting from the translation of a preprolipoprotein, which contains a signal peptide followed by a conserved four–amino acid sequence, [LVI][ASTVI][GAS]C, also known as the lipobox (14). After translation, the preprolipoprotein is secreted through the IM via the Sec or Tat pathways, followed by modification by three enzymes (Lgt, LspA, and *N*-acyl transferase [Lnt]) to generate the mature triacylated lipoproteins. First, Lgt recognizes the lipobox and catalyzes the transfer of diacylglyceryl (DG) from phosphatidylglycerol to the thiol group of the conserved cysteine residue in the lipobox sequence. The second enzyme, LspA, is an aspartyl endopeptidase, which cleaves off the signal peptide N terminal of the conserved diacylated +1 cysteine (15), and is the molecular target of the natural product antibiotics globomycin and myxovirescin (16–19). In gram-negative and high-GC gram-positive bacteria, a third enzyme, Lnt, catalyzes the addition of a third acyl chain to the amino group of the N-terminal cysteine via an amide linkage. Unlike *lgt* and *lspA*, *lnt* is dispensable for *A. baumannii* growth in vitro (20). In *A. baumannii*, mature triacylated lipoproteins destined for the OM are recognized by the localization of lipoprotein (Lol) pathway DF complex (LolDF) (21), analogous to the LolCDE adenosine triphosphate (ATP)–binding cassette transporter expressed in Enterobacteriaceae and *Pseudomonas* species.

In *E. coli*, resistance to inhibitors of LspA has been well studied and is mediated by deletion or decreased expression of the major OM lipoprotein, *lpp*. Lpp (also known as Murein lipoprotein or Braun's lipoprotein) is a small ∼8-kDa lipoprotein that is the most abundant OM protein in *E. coli* (∼500,000 molecules per cell) and that forms covalent interactions between the PGN layer and the OM. A third of all Lpp is covalently linked to PGN through a covalent interaction between the C-terminal lysine and the *meso*-diaminopimelic acid residue of the PGN layer (11, 22–26). *E. coli* mutants deficient in *lpp* exhibit increased OM permeability, leakage of periplasmic components, increased outer membrane vesicle (OMV) release, and increased sensitivity to complement-mediated lysis (27). Inhibitors of LspA (19, 28) and LolCDE (29, 30) lead to the mislocalization and accumulation of PGN-linked DG-modified Lpp in the IM, resulting in *E. coli* cell death. Consequently, *lpp* deletion and decreased expression are major mechanisms of *E. coli* resistance to inhibitors of LspA and LolCDE (19, 28–32). Given that inhibitors of lipoprotein biosynthesis have minimal activity against *A. baumannii* strains, which do not express Lpp homologs, the resistance mechanisms to LspA inhibitors in *A. baumannii* remain unknown.

In this study, we describe a potent globomycin analog, G5132, with increased antibacterial activity against multiple laboratory and clinical antibiotic-resistant *A. baumannii* isolates. Resistance to G1532 in *A. baumannii* maps to a single hypothetical gene encoding a putative lipoprotein. We confirm that this gene encodes an abundant alanine-rich lipoprotein, which we have renamed LirL (prolipoprotein signal peptidase inhibitor resistance lipoprotein), and describe the initial characterization of this lipoprotein and its role in *A. baumannii* growth and virulence.

Results

G5132 Is a Potent Globomycin Analog. Given that globomycin has poor antibacterial activity against wild-type Enterobacteriaceae strains, we sought to optimize the globomycin chemical structure to improve activity against Enterobacteriaceae and expand that activity more broadly across other gram-negative pathogens, including *A. baumannii*. The globomycin structure is modular, composed of five amino acids joined in a macrocycle through a β-hydroxy acid–containing lipophilic tail (Fig. 1*A*). The identification of optimized globomycin analogs through structure-based design has been described in detail elsewhere (33). Compound G5132 was identified based on its increased antibacterial activity against *E. coli* and contains modifications at five of these six segments. The globomycin amino acids serine, *allo*-isoleucine, and *N*-methyl-leucine were replaced with (*S*)-2,3-diaminopropionic acid (Dap), cycloheptylglycine, and *N*-methyl-norvaline at positions a, b, and c, respectively (Fig. 1 *A*, *a*–*c*). Additionally, the flexible lipophilic *n*-hexyl aliphatic group at position d (Fig. 1 *A*, *d*) was replaced with a bulky and conformationally constrained *exo*-norbornyl–containing moiety. The *allo*-threonine residue at position e (Fig. 1 *A*, *e*) was modified to contain a *trans*-amino-cyclobutyl ether, with this positive charge hypothesized to enhance accumulation inside the cells (34). These modifications in G5132 served to enhance whole-cell activity compared with globomycin (Table 1), leading to bactericidal activity in *A. baumannii* American Type Culture Collection (ATCC) 17978 (Ab17978) (Fig. 1*B*) and loss of cytoplasmic green fluorescent protein (GFP) from Ab17978 containing a plasmid expressing GFP (pWH-*sfGFP*) (Fig. 1*C*) after treatment with G5132. Electron microscopy revealed significant G5132-induced defects in cellular morphology, including loss of cytoplasmic contents and thinning of the glycocalyx (*SI Appendix*, Fig. S1). Compared with globomycin, G5132 showed a >8-fold reduced minimal inhibitory concentration (MIC) against wild-type *A. baumannii* strains Ab17978 and Ab19606 as well as >10-fold reduced MIC against *E. coli*, *Enterobacter cloaceae*, and *K. pneumoniae* strains (Table 1). G5132, like the parent globomycin, showed a high MIC against *S. aureus* USA300, consistent with data demonstrating that *lspA* is dispensable for *S. aureus* growth in vitro (35, 36). Importantly, G5132 is equally potent against laboratory strains and clinical *A. baumannii* isolates, including the antibiotic-resistant isolates Centers for Disease Control and Prevention (CDC) 0052, 0035, and 0070, which express the plasmid-borne β-lactamases belonging to the oxacillinase (OXA) family of β-lactamases known to confer high levels of carbapenem resistance (37) and other gentamicin-resistant *A. baumannii* clinical isolates (International Health Management Associates [IHMA] 941383 and 952682) (Table 1). Given that antibacterial agents that target single enzymes essential for bacterial growth are subject to the significant selection pressure leading to the development of high-level resistance, we profiled the resistance mechanisms to G5132 in wild-type *A. baumannii* strains.

G5132 Resistance in *A. baumannii* Maps to a Putative Alanine-Rich Lipoprotein. Resistance to globomycin or improved analogs of globomycin in Enterobacteriaceae is known to be mediated either by *lspA* overexpression caused by unstable heteroresistance or by decreased expression or deletion of the major OM lipoprotein, *lpp*. As expected, overexpression of *lspA* derived from either *A. baumannii* ($lspA^{Ab}$) or *E. coli* ($lspA^{Ec}$) conferred resistance to G5132 in the clinical uropathogenic *E. coli* isolate, CFT073 (*SI Appendix*, Table S1). Given that *A. baumannii* does not express an *lpp* homolog, we set out to empirically identify the mechanisms of G5132 resistance in *A. baumannii*. Resistance selections were performed in three *A. baumannii* isolates: Ab17978, Ab19606, and the highly virulent clinical isolate AB5075-UW (AB5075). Independent colonies growing on agar plates containing

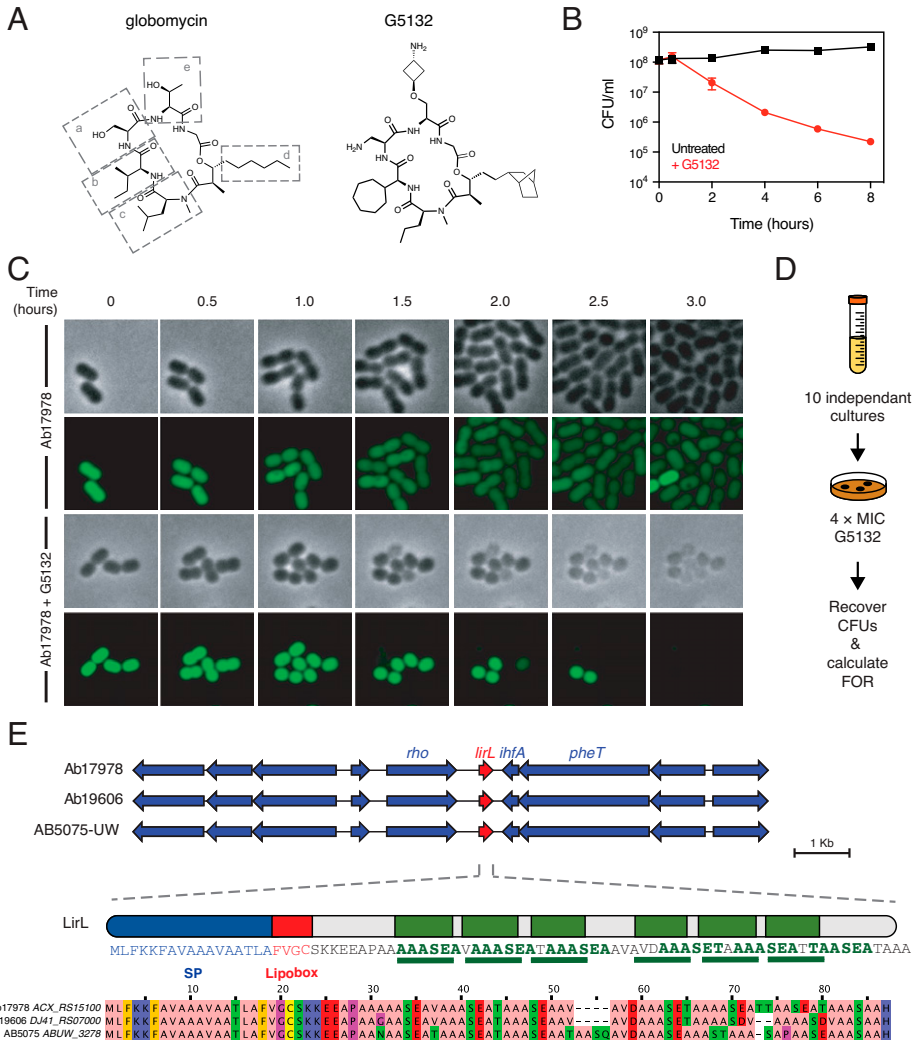

Fig. 1. Resistance to G5132, an improved globomycin analog, in *A. baumannii* maps to a single hypothetical gene. (*A*) Chemical structures of globomycin and G5132 showing modified side chains at positions "a" (*A*, *a*; serine to Dap), "b" (*A*, *b*; *allo*-isoleucine to cyloheptylglycine), "c" (*A*, *c*; *N*-methyl-leucine to *N*-methyl-norvaline), and "e" (*A*, *e*; *allo*-threonine residue to a *trans*-amino-cyclobutyl ether). The flexible lipophilic *n*-hexyl aliphatic group at position "d" (*A*, *d*) is replaced with an *exo*-norbornyl–containing moiety. (*B*) G5132 is bactericidal against *A. baumannii* strain Ab17978. Ab17978 was left untreated (black) or was treated with 4× MIC of G5132 (red), and CFUs were enumerated at various times posttreatment. Raw CFUs per milliliter (mean ± SD) are plotted from an experiment performed in triplicate. (*C*) Time-lapse microscopy of Ab17978 treated with G5132. GFP-expressing Ab17978 was left untreated or was treated with 4× MIC of G5132 for 3 h. Phase contrast and fluorescence microscopy images at 30-min intervals are presented. (*D*) Schematic representing the strategy to select for G5132-resistant mutants. Ten independent overnight cultures of *E. coli* CFT073, *K. pneumoniae* 700603, *E. cloacae* 13047, Ab17978, and Ab19606 were spread on cation-adjusted Mueller–Hinton agarose plates containing G5132 at 4× MIC. For AB5075, only three independent overnight cultures were tested due to compound limitations. (*E*) Resistance to G5132 in *A. baumannii* maps to a single gene. Gene maps for G5132-resistant strains depicting the gene (renamed *lirL*) and ClustalWS alignment of the *lirL* protein coding region from Ab17978, Ab19606, and AB5075. Putative signal peptide (SP; blue), lipobox (red), and alanine-rich repetitive regions (green) are depicted.

4× MICs of G5132 were picked for further analyses (Fig. 1*D*). Ab19606 and AB5075 strains showed >5,000-fold higher frequency of resistance (FOR) compared with Ab17978, which itself was lower than that seen in *E. coli* and *K. pneumoniae* (*SI Appendix*, Table S2). We examined their genomes to determine if this was due to the presence of additional *lspA* genes in Ab19606 and AB5075. Besides the essential *lspA* gene, Gallagher et al. (38) have identified a viable AB5075 mutant (AB09635) containing an ISPpu12 transposable element in the ABUW_3663 locus (ABUW_RS17835), which is also annotated as a signal peptidase II. Genomic sequence analyses revealed that both AB5075 and AB19606 encode two *lspA* genes: the essential *lspA* gene, which is flanked by *ileS* and *fkpB* as in *E. coli*, and a second *lspA* ortholog (*ABUW_3663* and *DJ41_RS04640* in AB5075 and Ab19606, respectively). To determine if the extra *lspA* copy contributes to the higher FOR detected in Ab19606 and AB5075, we used an engineered mutant Ab19606, which had *DJ41_RS04640* deleted (Ab19606Δ*DJ41_RS04640*), and AB09635, an AB5075 mutant containing a transposon in the ABUW_3663 locus (38). G5132 FOR in wild-type Ab19606 and Ab19606Δ*DJ41_RS04640* was similar (*SI Appendix*, Table S2). Although G5132 FOR in AB09365 (AB5075Δ*ABUW_3663*) was ∼8-fold lower than that in the parental AB5075 strain, it was still ∼1,100-fold higher than that seen in Ab17978, suggesting that the presence of an extra *lspA* copy does not significantly affect G5132 FOR.

All the independent colonies growing on agar plates containing 4× MICs of G5132 were more than eightfold resistant to G5132 (*SI Appendix*, Table S3). To map mutations conferring G5132 resistance, we performed whole-genome sequencing (WGS) of Ab17978 and Ab19606 G5132-resistant ($G5132^R$) colonies. WGS identified mutations in the hypothetical genes (*ACX_RS15100* and *DJ41_RS07000* in Ab17978 and Ab19606,

Table 1. MICs of globomycin, G5132, gentamicin, and carbenicillin against a panel of clinical *A. baumannii* and other gram-negative bacterial species

Name	Source	Bacterial species	Known acquired resistance*	MIC (μg/mL)			
				Globomycin	G5132	Gentamicin	Carbenicillin
941383	IHMA	*A. baumannii*		>65.6	8.3	>500	>500
952682	IHMA	*A. baumannii*		>65.6	5.6	>500	>500
945295	IHMA	*A. baumannii*		>65.6	5.6	125	>500
937775	IHMA	*A. baumannii*		>65.6	16.7	2.0	>500
0052	CDC	*A. baumannii*	OXA-23	>65.6	5.6	187.5	>500
0035	CDC	*A. baumannii*	OXA-72, OXA-23	65.6	5.6	62.5	>500
0070	CDC	*A. baumannii*	OXA-58	>65.6	5.6	375	>500
17978	ATCC	*A. baumannii*		>65.6	8.3	4	62.5
19606	ATCC	*A. baumannii*		>65.6	8.3	62.5	31.3
AB5075-UW	ATCC	*A. baumannii*		>65.6	11.1	>500	>500
941383	IHMA	*A. baumannii*		>65.6	5.6	>500	>500
952682	IHMA	*A. baumannii*		>65.6	5.6	125	>500
25922	ATCC	*E. coli*		49.2	1.4	1.5	62.5
700928	ATCC	*E. coli*		32.8	1.4	2.0	15.6
13407	ATCC	*E. cloacae*		>65.6	5.6	1.5	375
222	ATCC	*E. cloacae*		65.6	1.4	<0.5	4.0
13883	ATCC	*K. pneumonia*		>65.6	5.6	<0.5	>500
700721	ATCC	*K. pneumonia*		65.6	5.6	62.5	>500
USA300	NARSA	*S. aureus*		>65.6	88.8	<0.5	125

*MIC measured by the CDC.NARSA (Network on Antimicrobial Resistance in *Staphylococcus aureus*).

respectively) that were absent in their parental strains (*SI Appendix*, Table S3). Sequence alignment of *ACX_RS15100* and *DJ41_RS07000* indicated that they both encode the same putative protein with ∼89% identity (Fig. 1*E* and *SI Appendix*, Table S3). Using PCR to sequence the homologous gene in AB5075 (*ABUW_3278*), we identified similar mutations in the same gene in G5132^{R} AB5075 (*ABUW_3278*) that were absent in the parental AB5075 strain (Fig. 1*E* and *SI Appendix*, Table S3), suggesting that this gene contributes to G5132 resistance. The translated amino acid sequence of this gene predicts a small, highly alanine-rich (48%) protein containing 81– to 86–amino acid residues with a predicted molecular weight of ∼8.9 to 9.5 kDa and an isoelectric point of ∼4.52 (Fig. 1*E*). The putative protein sequence contains a hydrophobic signal peptide followed by a lipobox sequence (FVGC), which contains a cysteine residue known to be modified in bacterial lipoproteins (39). The lipobox cysteine is followed by an Ser residue, thought to be important for OM targeting (40). Given the homology between *ACX_RS15100*, *DJ41_RS07000*, and *ABUW_3278*, we henceforth refer to these genes as *lirL*.

All the mutations identified in G5132^{R} strains were localized within the putative signal peptide upstream of the lipobox and included insertion–deletion mutations and amino acid substitutions (Table 2 and *SI Appendix*, Table S3). The most frequent types of mutations were insertions (FAVAA, AAV, or VA) or small amino acid deletions. Protein homology searches using Basic Local Alignment Search Tool (BLAST) with default parameter settings did not identify *lirL* homologs in the Enterobacteriaceae family, but *lirL* homologs were identified in all sequenced *A. baumannii* isolates tested, including CDC *A. baumannii* clinical isolates, and in certain *Pseudomonales*, *Serratia*, and *Parabulkhoderia* isolates (*SI Appendix*, Fig. S2). While the N-terminal region of the protein is fully conserved across all *A. baumannii* isolates (Fig. 1*E* and *SI Appendix*, Fig. S2*B*), the C-terminal region is more variable and contains approximately six alanine-rich repetitive motifs [AAAS(E/D)(V/A/T)]. To determine if the G5132^{R} variants are recessive to wild-type LirL when coexpressed, we expressed hemagglutinin (HA)–tagged *lirL* in two G5132^{R} strains expressing a single genomic copy of histidine (his)–tagged G5132^{R}-1 or G5132^{R}-8 (Ab17978$lirL_{His}^{G5132R\text{-}1}$ and Ab17978$lirL_{His}^{G5132R\text{-}1}$). Expression of wild-type *lirL* in G5132^{R} cells resensitized cells to G5132, similar to that seen in parental strains (*SI Appendix*, Table S4). Consistent with these data, overexpression of wild-type but not G5132^{R}-1 *lirL* increased sensitivity to G5132 in Ab17978 (*SI Appendix*, Table S4). Cumulatively, these data demonstrate that the G5132^{R} *lirL* mutants are recessive to wild-type *lirL* when coexpressed. In order to further characterize LirL, we first decided to confirm if *lirL* encodes a lipoprotein.

***lirL* Encodes a Larger than Predicted Lipoprotein.** To determine if *lirL* encodes a lipoprotein, we generated an antibody against the putative open reading frame. We expressed and purified recombinant LirL (Ser_{22}-His_{83}) with N-terminal and C-terminal his-tag and flag-tag (His_6-LirL-Flag), respectively, from insect cells and immunized rabbits to generate an anti-LirL polyclonal antibody. Western blot analyses performed on wild-type Ab17978 and Ab19606 cell lysates resulted in detection of a higher than expected ∼20- to 21-kDa protein that was absent in the corresponding *lirL* deleted strains (Ab17978Δ*lirL* and Ab19606Δ*lirL*), and complementation with a plasmid expressing *lirL* resulted in expression levels similar to that seen in the parental strains (Fig. 2*A*). Recombinant LirL also migrated at higher than expected molecular weights and was detected as either a single or double species depending on the type of SDS-PAGE (*SI Appendix*, Fig. S3*A*). However, intact liquid chromatography–mass spectrometry (LC/MS) analysis confirmed that the molecular weight of recombinant LirL (8,747.45 Da) matched the theoretical weight (8,705.07 Da) and size exclusion chromatography–multiple angle laser light scattering (SEC-MALS) confirmed it to be a monomer (*SI Appendix*, Fig. S3 *B* and *C*). Transcomplementation of Ab17978Δ*lirL* with a C-terminally hemagglutinin (HA)–tagged *lirL* led to increased G5132 sensitivity (*SI Appendix*, Table S5),

Table 2. MICs of G5132 and other antibiotics against G5132-resistent and Δ*lirL A. baumannii* strains

	MIC (n = 2)					
	G5132 (μg/mL)	NaCl (%)	Vancomycin (μg/mL)	Amikacin (μg/mL)	Gent (μg/mL)	Levo (μg/mL)
Ab17978	5.6	5	>148.6	4.9	7.0	0.4
Ab17978Δ*lirL*	66.6	5	>148.6	2.4	2.4	0.1
Ab17978Δ*lirL*+pWH	66.6	5	>148.6	1.3	2.4	0.2
Ab17978Δ*lirL:* pWH-*lirL*^{Ab17978}	2.8	5	>148.6	4.9	4.6	0.3
Ab17978Δ*lirL:* pWH-*lirL-ΔR*^{Ab17978}	5.6	—	—	—	—	—
Ab17978 G5132^{R}-1	>88.8	5	>148.6	4.9	7.0	0.2
Ab17978 G5132^{R}-2	>88.8	5	>148.6	3.7	4.6	0.1
Ab19606	8.3	10	>148.6	78.2	—	0.4
Ab19606Δ*lirL*	>88.8	5	>148.6	14.7	—	0.4
Ab19606Δ*lirL*+pWH	>88.8	5	>148.6	29.3	—	0.6
Ab19606Δ*lirL:* pWH-*lirL*^{Ab19606}	5.6	5	>148.6	78.2	—	0.4
Ab19606 G5132^{R}-9	>88.8	10	>148.6	58.7	—	0.6
Ab19606 G5132^{R}-10	>88.8	10	>148.6	78.2	—	0.6
Ab19606 G5132^{R}-11	>88.8	10	>148.6	78.2	—	0.4
Ab19606 G5132^{R}-12	>88.8	10	>148.6	78.2	—	0.4

— indicates not determined.

similar to that seen with wild-type *lirL*. Boiling or treating the cell lysate with β-mercaptoethanol did not alter the SDS-PAGE migration of LirL (*SI Appendix*, Fig. S3*D*).

To determine the actual mass of full-length LirL and if LirL was indeed a lipoprotein, we engineered Ab17978 to express a single genomic copy of his-tagged *lirl* (Ab17978*lirL*$_{His}$). No significant difference in SDS-PAGE migration was observed between LirL and LirL-His, apart from the latter migrating slower due to the presence of the his-tag (*SI Appendix*, Fig. S3*E*). LirL-his was then purified from untreated and G5132-treated Ab17978*lirL*$_{His}$, and mass spectrometry was performed. If LirL is a lipoprotein, we would expect to detect accumulation of higher–molecular weight LirL intermediates corresponding to a DG-modified prolipoprotein intermediate (DG-proLirL), as has been demonstrated for Lpp in *E. coli* with another globomycin analog (32). Mass spectrometry analyses of purified LirL-His revealed multiple LirL species with molecular weights in the range of 12 to 13.5 kDa, much higher than the ∼7.2-kDa theoretical weight of triacylated LirL (Fig. 2*B* and *SI Appendix*, Fig. S3*F*). G5132 treatment led to the accumulation of higher–molecular weight LirL species and resulted in detection of higher–molecular weight intermediates of Pal and LirL, corresponding to DG-proPal and DG-proLirL, respectively (Fig. 2 *B* and *C* and *SI Appendix*, Fig. S3*G*). Unfortunately, we were unable to resolve these higher than predicted LirL species in either untreated or G5132-treated cells. These data suggested that LirL expressed in *A. baumannii* is very likely a lipoprotein, and although LirL may migrate aberrantly in SDS-PAGE, it is likely posttranslationally modified to as yet uncharacterized moieties.

Given that alanine-rich regions have been demonstrated to lead to protein misfolding or aggregation (41), which could pose challenges for further characterization of full-length LirL, we engineered Ab17978Δ*lirL* to only express HA-tagged truncated LirL mutants containing either no repeats (LirL-ΔR) or containing one, two, or three repeats (LirL-R1, LirL-R12, and LirL-R123, respectively) (Fig. 2*D*). The theoretical expected molecular weight of triacylated LirL-ΔR is ∼2.9 kDa, after cleavage of the signal peptide (2.026 kDa) by LspA and the addition of palmitic acid (238 Da) by Lnt (Fig. 2 *D*, *Right*). Transcomplementation of Ab17978Δ*lirL* with the *lirL*-ΔR truncated variant resensitized cells to G5132, similar to that seen with the full-length LirL (Table 2). Triacylated LirL-ΔR, which should theoretically be ∼2.9 kDa, was migrating closer to ∼6 kDa in SDS-PAGE (Fig. 2*E*). G5132 treatment of Ab17978 expressing LirL-ΔR resulted in accumulation of a higher-molecular weight species consistent with DG-modified proLirL-ΔR (DG-proLirL-ΔR). The detection of DG-proLirL-ΔR was dependent on the presence of the conserved lipobox cysteine as no higher–molecular weight species were detected in cells only expressing LirL-ΔR containing a C21A mutation (LirL-ΔR^{C21A}), which cannot be modified by the lipoprotein biosynthetic enzymes (Fig. 2*E*). Treatment of cells with G5132 expressing any of the LirL truncated mutants also led to similar accumulation of what are expected to be DG-modified intermediates, although clearly, identifying the DG-modified forms became increasingly challenging as the number of alanine-rich repeats increased (Fig. 2*E*). To provide definitive proof that LirL-ΔR was indeed a lipoprotein, we purified his-tagged LirL-ΔR from untreated or G5132-treated Ab17978 containing pWH-*lirL*-ΔR-His and performed mass spectrometry analyses. Mass spectrometric analyses confirmed that the expected ∼2.9-kDa form in untreated cells corresponds to monomeric triacylated mature LirL-ΔR (Fig. 2*E* and *SI Appendix*, Fig. S4*A*). G5132 treatment led to the accumulation of an ∼4.7-kDa form corresponding to DG-proLirL-ΔR (Fig. 2*E* and *SI Appendix*, Fig. S4*A*). We also detected accumulation of additional DG-proLirL-ΔR species containing a formyl-methionine (fMet) and/or a two-carbon-longer acyl tail attached to the lipobox cysteine (+28 Da). Cumulatively, these data conclusively demonstrate that *A. baumannii* LirL-ΔR is a lipoprotein.

LirL Is a Highly Abundant IM Lipoprotein That Is Not Covalently Linked to PGN. Given Lpp is a highly abundant *E. coli* lipoprotein, we attempted to quantitate the levels of LirL in *A. baumannii*. Recombinant LirL was used as a standard curve and compared with the level of LirL detected in Ab17978*lirL* lysate by western blot analyses. While the measured recombinant LirL molecular weight is ∼8.7 kDa, we used the most abundant peak (∼12.4 kDa) detected from our mass spectrometry analyses (*SI Appendix*, Fig. S3*F*) for our calculations. Based on quantitation of the LirL western blot, we estimate that there are ∼10^6 LirL molecules per colony forming unit (CFU) of Ab17978 (*SI Appendix*, Fig. S4*B*).

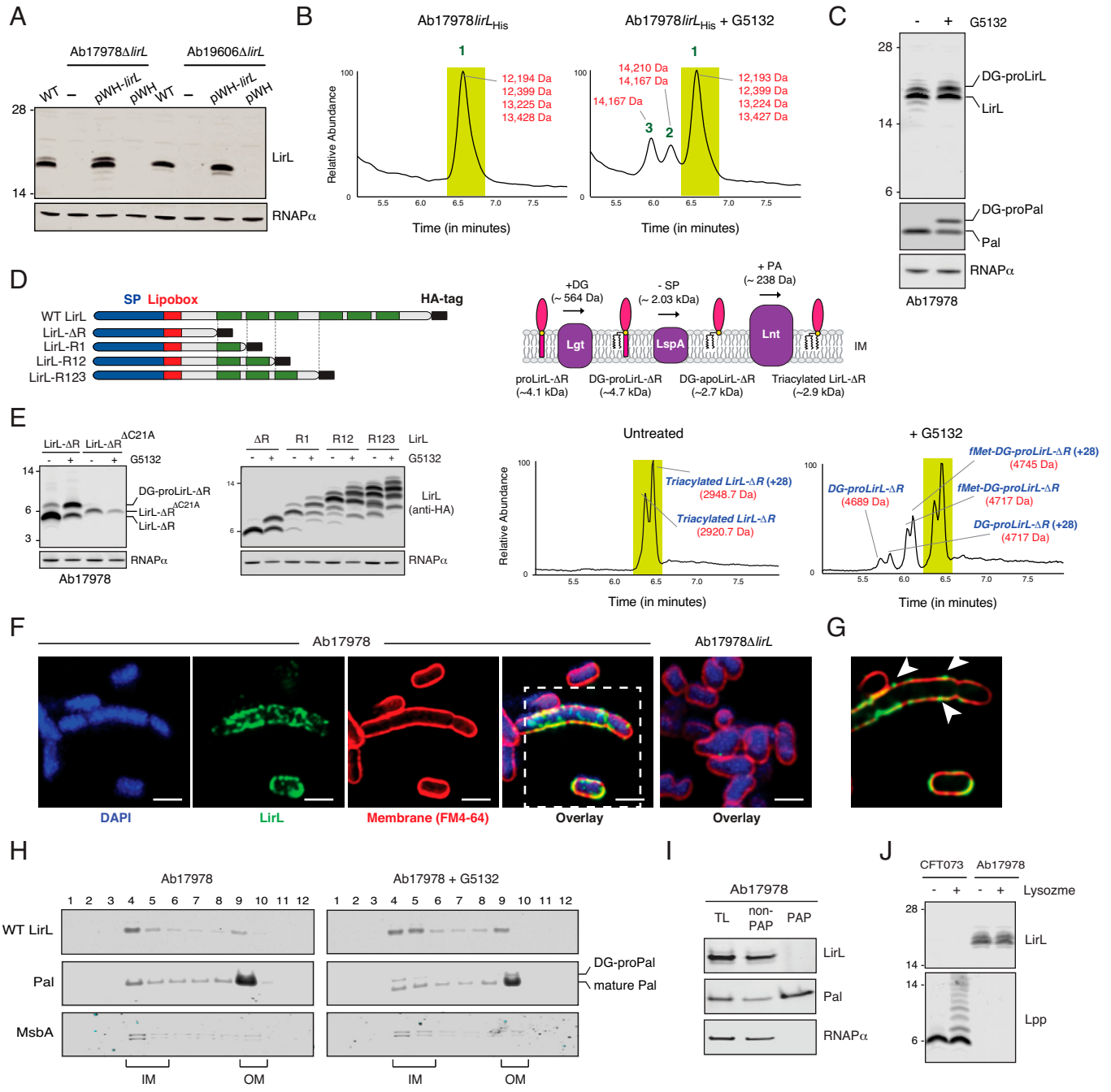

Fig. 2. *lirL* encodes an IM lipoprotein. (*A*) LirL expression in wild-type (WT) Ab19606 and Ab17978 total cell lysates demonstrated by western blot analysis. As controls, total cell lysates from *lirL* deletion strains (Ab17978Δ*lirL* and Ab19606Δ*lirL*) either noncomplemented (−) or complemented with empty plasmid (pWH) or plasmid expressing *lirL* (pWH-*lirL*) were tested for LirL protein expression. RNAPα was used as a loading control for this and subsequent western blots. Molecular weight markers are depicted to the left of the blots. (*B*) LC-UV-MS analysis of full-length his-tagged LirL (LirL-his) purified from untreated and G5132-treated cells Ab17978 cells expressing a single genomic copy of his-tagged *lirl* (Ab17978*lirL*$_{His}$). (*C*) Western blot analysis of total cell lysates from untreated (−) or G5132-treated (+) Ab17978 cells expressing his-tagged Pal, which was used as a control demonstrating inhibition of LspA. (*D*) Truncated mutant LirL isoforms and predicted molecular weights of LirL-ΔR lipoprotein intermediates. DG, signal peptide (SP), and palmitic acid (PA) in Ab17978 cells untreated or treated with 44.4 μg/mL G5132. *D*, *Left* schematically depicts the HA-tagged LirL truncated variants containing no repeats (LirL-ΔR) or one, two, or three repeats (LirL-R1, LirL-R12, or LirL-R123, respectively). *D*, *Right* depicts the predicted intermediates of the LirL-ΔR mutant. (*E*) The LirL-ΔR mutant is a lipoprotein. *E*, *Left* shows the expected shift in SDS-PAGE migration after G5132 treatment. Total cell lysates from untreated (−) or 44.4 μg/mL G5132-treated (+) Ab17978Δ*lirL* complemented with plasmids expressing LirL-ΔR^{C21A}, LirL-ΔR, LirL-R1, LirL-R12, or LirL-R123 were subjected to western blot analysis. The various LirL-ΔR intermediates including DG-proLirL-ΔR are depicted. *E*, *Right* represents LC-UV-MS analysis of LirL-ΔR purified from untreated and G5132-treated Ab17978Δ*lirL* cells only expressing his-tagged LirLΔR. Accumulation of DG-proLirLΔR with or without an N-terminal *fMet* is detected in the G5132-treated cells. The +28-Da peak represents DG-proLirLΔR likely modified with acyl tails containing two additional carbons (CH_2-CH_2). (*F* and *G*) Detection of LirL in WT Ab17978 cells by confocal microscopy. The 3D reconstruction (*F*) and single *z*-stack (*G*) images are presented to denote membrane-specific punctate staining (arrows) using the anti-LirL polyclonal antibody. Control Ab17978Δ*lirL* cells showed no LirL staining. Membranes and DNA are stained with FM4-64 [*N*-(3-triethylammoniumpropyl)-4-(6-(4-(diethylamino) phenyl) hexatrienyl) pyridinium dibromide; red] and DAPI (4′,6-diamidino-2-phenylindole; blue), respectively. (Scale bars: 2 μm.) (*H*) Isopycnic sucrose gradient centrifugation of total membranes isolated from untreated or G5132-treated Ab17978 cells. IM (fractions 4 and 5) and OM (fraction 9) are depicted in the figure. (*I*) LirL is not detected in the PGN-associated fraction in Ab17978. PAP and non-PAP fractions were separated from Ab17978 cells expressing his-tagged *pal*. Total lysates (TLs) were used as a comparison. RNAPα and Pal were used as controls for bacterial proteins expected to be detected in the non-PAP and PAP fractions, respectively. (*J*) SDS-PAGE migration of LirL is not sensitive to lysozyme treatment. Ab17978 and CFT073 cell lysates were treated with lysozyme prior to running western blot analyses using anti-Lpp and anti-LirL antibodies.

These levels are consistent with those measured for *E. coli* Lpp, suggesting that LirL is a highly abundant *A. baumannii* lipoprotein.

Since bacterial lipoproteins are localized to the IM or OM, we assessed whether LirL was membrane localized. Using the anti-LirL polyclonal antibody, we demonstrated that full-length LirL expression was localized to specific cellular domains, as detected in 3D reconstructed confocal microscopy images of wild-type Ab17978 but not in Ab17978Δ*lirL* cells (Fig. 2*F*). Further analysis of single *z*-stack images confirmed that LirL localized to the bacterial cell membrane (Fig. 2*G*). In order to localize LirL to specific cell membranes, we separated Ab17978 IM and OM using isopycnic sucrose gradient centrifugation, as measured by probing the fractions for MsbA (IM protein) and Pal (OM lipoprotein) (Fig. 2*H*). LirL was primarily enriched in the IM fractions, but low levels were also detected in the OM fraction. G5132 treatment led to a modest accumulation of DG-proPal and LirL/DG-proLirL (Fig. 2*H*). The detection of DG-proPal in the OM fraction in G5132-treated cells is likely an artifact due to incomplete membrane separation. These data demonstrate that LirL is primarily localized to the IM.

While the positively charged ε-amino group of the C-terminal lysine in Lpp is covalently linked to PGN in *E. coli*, we used multiple approaches to determine if the detection of higher than expected molecular weight LirL species suggested that LirL is covalently associated with PGN. As LirL contains a C-terminal histidine containing a positively charged imidazole group, which is a catalytic residue frequently found in the active sites of enzymes (42) and can covalently link to other amino acids (43), we asked if the C-terminal histidine was critical for G5132 resistance. We first confirmed that expression of both *lirL* and $lirL_{HA}$ resensitized Ab17978Δ*lirL* to G5132 (*SI Appendix*, Table S5). We then generated strains expressing a single copy of HA-tagged *lirL* (Ab17978$lirL_{HA}$) or a mutant with the C-terminal histidine deleted (Ab17978$lirL\Delta H_{HA}$) and tested sensitivity to G5132. Deletion of the C-terminal histidine in LirL did not lead to G5132 resistance (*SI Appendix*, Table S5). Second, we used an SDS solubilization protocol to enrich peptidoglycan-associated proteins (PAPs), which have been previously used in *E. coli* (44, 45). While the *A. baumannii* OM lipoprotein Pal and the cytoplasmic RNA polymerase-α (RNAPα) protein were detected in the PAP and non-PAP fractions, respectively, LirL was undetectable in the PAP fraction (Fig. 2*I*). Last, we determined if lysozyme treatment altered the SDS-PAGE migration of LirL. While lysozyme treatment of *E. coli* CFT073 led to the expected detection of covalent PGN-linked Lpp species, SDS-PAGE migration of LirL in Ab7978 was unchanged after lysozyme treatment (Fig. 2*J*). Cumulatively, our data demonstrate that LirL is not covalently linked to PGN.

Deletion of *lirL* Results in Morphological Defects, Increased Clearance by Macrophages, and Attenuated Virulence in Mice. To determine if G5132 resistance was mediated by loss-of-function mutations in *lirL*, we tested the sensitivity of Ab17978Δ*lirL* and Ab19606Δ*lirL* to G5132. Ab17978Δ*lirL* and Ab196060Δ*lirL* were as resistant to G5132 as the selected $G5132^R$ mutants, and transcomplementation of the two deletion strains with wild-type *lirL* led to increased G5132 sensitivity (Table 2). While *lirL* deletion resulted in a modest increase in sensitivity to amikacin, it did not lead to increased sensitivity to vancomycin, a gram-positive antibiotic that is unable to efficiently penetrate through the gram-negative OM (46). The Ab17978Δ*lirL* growth rate was decreased comparable with that of the wild-type Ab17978 in broth (Fig. 3*A*), and both Ab17978Δ*lirL* and Ab196060Δ*lirL* showed considerable morphological defects by electron microscopy and immunofluorescence staining (Fig. 3 *B* and *C*). Both Ab17978Δ*lirL* and Ab196060Δ*lirL* presented as smaller growing colonies on agar plates, which were rescued by complementation with a plasmid expressing *lirL* (*SI Appendix*, Fig. S5*A*). Deletion of *lirL* led to a globular phenotype, with occasional cells with absent cytoplasmic contents and an increase in the frequency of cells with incomplete cell separation and membrane indentations (Fig. 3 *B* and *C* and *SI Appendix*, Fig. S5*B*). Time-lapse fluorescence microscopy demonstrated that Ab17978Δ*lirL* cell division occasionally results in daughter cells that lose cytoplasm while maintaining an intact OM, resembling bacterial ghosts (Fig. 3*C*). These data suggest that although cell division can occur in the absence of *lirL*, the process is inefficient and can lead to slower growth in vitro and abnormal cell morphology, implicating LirL as a key factor involved in *A. baumannii* growth and cell division.

We next performed a number of studies to determine the effect of *lirL* deletion on *A. baumannii* pathogenesis and immune clearance. Given that *E. coli* lipoproteins are critical for serum resistance (47, 48), we sought to determine if LirL was important for preventing serum killing of *A. baumannii*. While normal human serum (nHS) had no significant effect on wild-type Ab17978, incubation of *lirL*-deleted cells with nHS but not heat-inactivated human serum (HIHS) led to significant loss of viability (Fig. 3*D*). The effect of nHS on Ab17978Δ*lirL* viability was prevented after complementation with *lirL* (Fig. 3*D*). A similar, albeit more profound, loss in viability was detected in cells lacking *lnt*, the third enzyme involved in lipoprotein biosynthesis, consistent with the role of lipoproteins in serum resistance in gram-negative bacteria (Fig. 3*D*). Given that deficiency of the *E. coli* lipoproteins Lpp and Pal results in an increased production of OMVs (49), we asked whether deficiency of *lirL* in *A. baumannii* affected OMV formation. Ab17978Δ*lirL* cells produced significantly higher levels of OMV compared with Ab17978 (Fig. 3*E*). We also observed increased macrophage clearance of Ab17978Δ*lirL* compared with Ab17978 (Fig. 3*F*). Lastly, Ab17978Δ*lirL* was highly attenuated in a pneumonia mouse model, comparable with the *lnt* deleted strain (Fig. 3*G*). Taken together, our data suggest that LirL plays an important role in *A. baumannii* growth, serum resistance, and virulence.

LirL Does Not Functionally Rescue Lack of *lpp* in *E. coli*. *lirL* and *lpp* deletions in *A. baumannii* and *E. coli*, respectively, lead to increased serum sensitivity and thinning of the glycocalyx. To determine if LirL is functionally similar to Lpp, we engineered CFT073Δ*lpp* to express either *lirL* or *lpp* (*SI Appendix*, Fig. S6*A*). Since *lpp* deletion in *E. coli* CFT073 results in serum sensitivity (48), we tested the ability of *lirL* to increase serum resistance of CFT073Δ*lpp*. Expression of *lpp* but not *lirL* resulted in increased serum resistance of CFT073Δ*lpp* (*SI Appendix*, Fig. S6*B*). While this could be due to inappropriate membrane localization of LirL in *E. coli*, we engineered CFT073Δ*lpp* to express LirL chimeras that had their endogenous signal sequence, lipobox, and +2 residues replaced with comparable sequences from an *E. coli* IM lipoprotein, NlpA ($nlpA_{SP}$ *lirL*), or an OM lipoprotein, Lpp (lpp_{SP} *lirL*). Similar to that seen with cells expressing wild-type *lirL*, expression of $nlpA_{SP}$ *lirL* or lpp_{SP} *lirL* did not lead to increased serum resistance of CFT073Δ*lpp*, suggesting that LirL cannot functionally replace Lpp in *E. coli*. As G5132 treatment also leads to the accumulation of DG-proLirL in *A. baumannii* cells, the question still remained as to whether

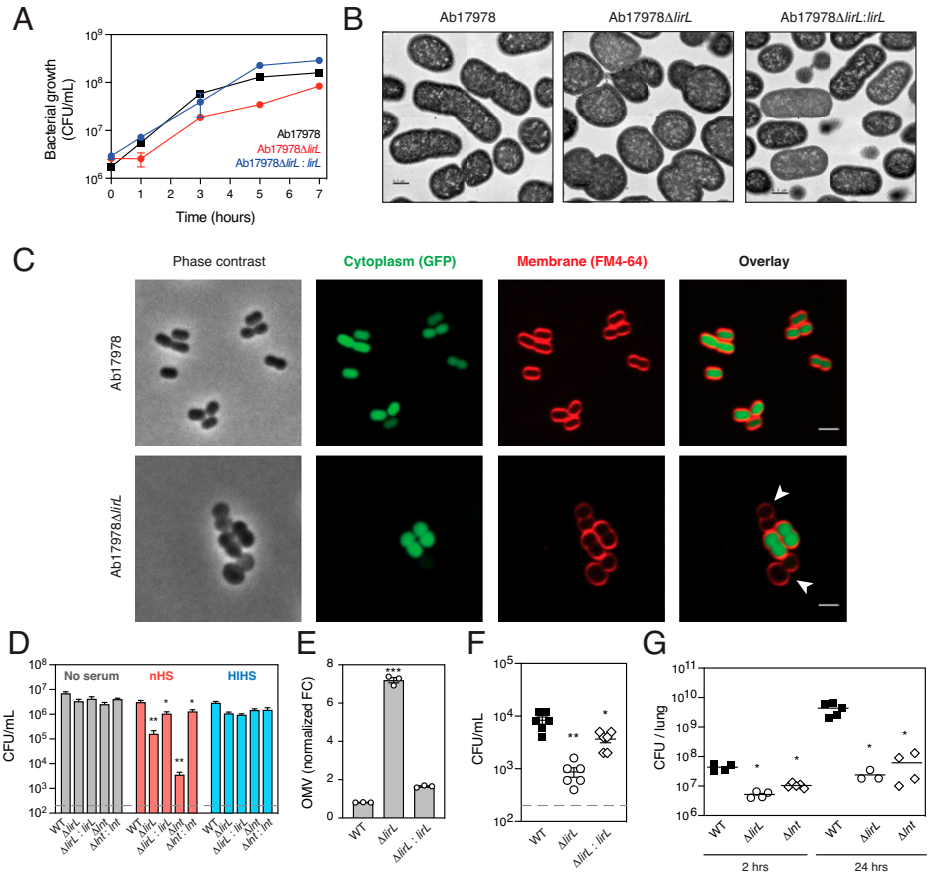

Fig. 3. LirL is critical for cellular morphology, serum resistance, decreased macrophage clearance, and virulence. (*A*) Ab17978, Ab17978Δ*lirL*, or Ab17978Δ*lirL* complemented with a plasmid expressing *lirL* (Ab17978Δ*lirL:lirL*) was grown over 7 h at 30 °C, and CFUs were enumerated at multiple time points. Data are representative of two independent experiments performed in duplicates (mean ± SD). (*B*) *lirL* deletion in Ab17978 cells leads to significant defects in cellular morphology by electron microscopy. Log-phase Ab17978, Ab17978Δ*lirL*, or Ab17978Δ*lirL:lirL* was processed for visualization by electron microscopy. (Scale bars: 0.5 μm.) (*C*) Immunofluorescence membrane staining using FM4-64 [*N*-(3-triethylammoniumpropyl)-4-(6-(4-(diethylamino) phenyl) hexatrienyl) pyridinium dibromide; red] of Ab17978 and Ab17978Δ*lirL* expressing GFP in the cytoplasm. Arrows represent ghost cells lacking cytoplasm. (Scale bars: 3 μm.) (*D*) Serum sensitivity of Ab17978Δ*lirL*. Ab17978 (wild type [WT]), Ab17978Δ*lirL* complemented with an empty plasmid (Δ*lirL*), and a plasmid expressing *lirL* (Δ*lirL:lirL*) were incubated with Mueller–Hinton broth, nHS, or HIHS for 1 h, and CFUs were enumerated. Ab17978Δ*lnt* (Δ*lnt*) and Ab17978Δ*lnt* complemented with a plasmid expressing *lnt* (Δ*lnt:lnt*) were used as controls. Data are plotted as mean ± SEM. These data are representative of two independent experiments performed in duplicate. $*P = 0.0087$; $**P = 0.0022$. (*E*) Increased OMV production by Ab17978Δ*lirL*. Supernatants were collected from Ab17978 (WT), Ab17978Δ*lirL* (Δ*lirL*), or Ab17978Δ*lirL* complemented with a plasmid expressing *lirL* (Δ*lirL:lirL*), and OMVs were isolated and quantitated as discussed in *Materials and Methods*. Quantitated OMVs were normalized to CFUs within each culture and plotted as fold change relative to CFU. Data are plotted as mean ± SEM. These data are representative of an experiment performed in triplicate. $***P < 0.0001$. (*F*) Ab17978Δ*lirL* cells are more sensitive to clearance by macrophages. Raw 264.7 macrophage cells were incubated with 10^7 CFU of Ab17978 (WT), Ab17978Δ*lirL* (Δ*lirL*), or Ab17978Δ*lirL* complemented with a plasmid expressing *lirL* (Δ*lirL:lirL*), and CFUs were enumerated at 24 h postincubation. Data are representative of two independent experiments each performed in triplicate. Pairwise comparisons were analyzed using an unpaired Mann–Whitney test. The gray dashed line represents the limit of detection (200 CFU/mL) for this experiment. $*P = 0.013$; $**P = 0.0022$. (*G*) Deletion of *lirL* leads to significant attenuation in virulence in a neutropenic lung infection model. Neutropenic Balb/c female mice were infected with Ab17978 (WT), Ab17978Δ*lirL* (Δ*lirL*), or Ab17978Δ*lnt* (Δ*lnt*), and CFU was enumerated at 2 and 24 h postinfection in lung homogenates by serial dilutions. Each symbol represents a single mouse. Overall *P* value for the ANOVA is $P < 0.0001$. Pairwise comparisons were analyzed using an unpaired Mann–Whitney test. *P* values for Δ*lirL* (2 h: $*P = 0.0286$; 24 h: $*P = 0.0357$) and Δ*lnt* (2 h and 24 h: $*P = 0.0159$) are denoted in the graph.

DG-proLirL accumulation and/or mislocalization account for the bactericidal effect of G5132 in *A. baumannii.*

Signal Peptide Mutations in G5132^R *A. baumannii* Lead to Less Efficient Processing of DG-proLirL by LspA. Given that the mutations conferring resistance to G5132 are very similar in all three tested *A. baumannii* strains, we used Ab17978 to better understand the mechanism of resistance to G5132. We picked two representative Ab17978 G5132^R clones G5132^R-1 and G5132^R-8, which contain an "AVAA" insertion and "AAA" deletion, respectively, in the LirL signal peptide. Unlike Ab17978Δ*lirL*, both G5132^R-1 and G5132^R-8 showed normal cellular morphology compared with Ab17978 (Fig. 4*A*). G5132^R mutants from both Ab17978 and Ab19606 expressed LirL to similar levels as their parental strains, although the G5132^R mutants expressed additional lower–molecular weight forms of LirL (Fig. 4*B*). Despite their normal cellular morphology, virulence of both G5132^R-1 and G5132^R-8 remained attenuated in the pneumonia infection model (Fig. 4*C*). A G14D mutation in the *E. coli* Lpp signal sequence has been demonstrated to lead to globomycin resistance by decreasing secretion through the IM, leading to accumulation in the soluble cytoplasmic fraction (50). To determine if G5132^R mutations lead to accumulation of soluble LirL, we fractionated Ab17978 and Ab17978-G5132^R-1 cell lysates containing plasmid expressing *pal-his* to generate soluble and insoluble fractions. Although Pal was primarily detected in the total cell lysates and insoluble fractions in both Ab17978 and Ab17978-G5132^R-1 (*SI Appendix*, Fig. S7*A*), no increased accumulation of LirL was detected in the Ab17978-G5132^R-1 soluble fractions compared with Ab17978 (*SI Appendix*, Fig. S7*A*). We then asked if DG-proLirL accumulation in the IM could be

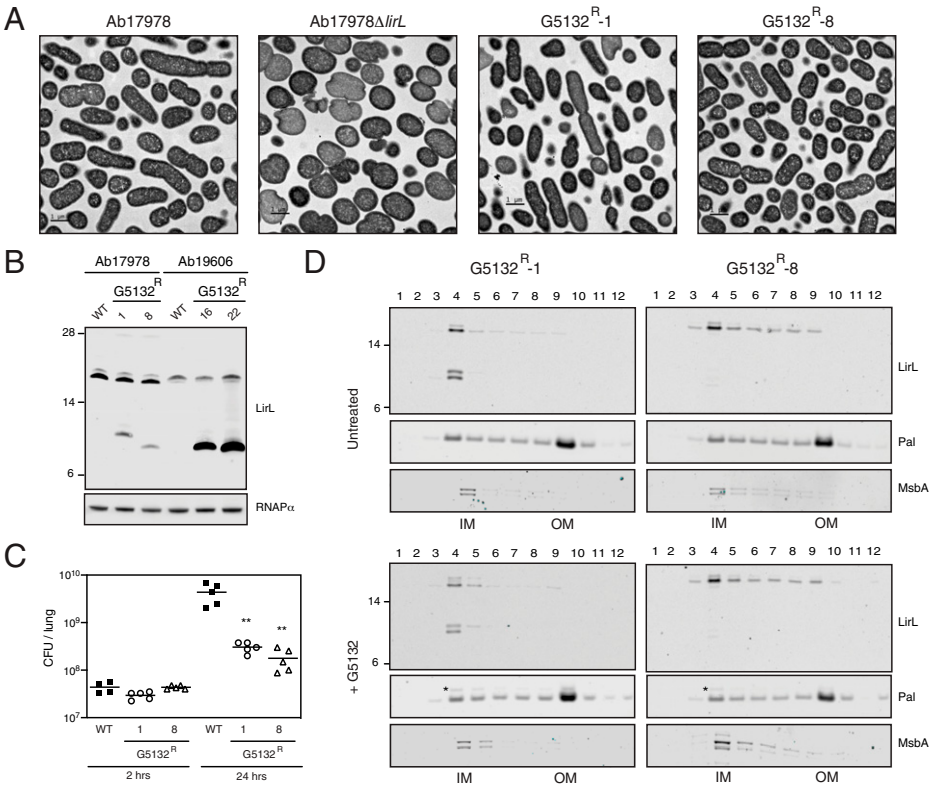

Fig. 4. G5132^R Ab17978 does not exhibit the morphology defect seen in Ab17978Δ*lirL* but is attenuated in virulence. (*A*) Log-phase Ab17978, Ab17978Δ*lirL*, and Ab17978 G5132^R isolates 1 and 8 were processed for visualization by electron microscopy. (Scale bars: 1 μm.) (*B*) LirL expression in representative Ab19606 and Ab17978 G5132^R isolates. Total cell lysates were analyzed by western blot analysis. RNAPα was used as a loading control. Molecular weight markers are depicted to the left of the blots. (*C*) Neutropenic Balb/c female mice were infected with wild-type (WT) Ab17978, G5132^R-1, and G5132^R-8 strains, and CFUs were enumerated at 2 and 24 h postinfection in lung homogenates by serial dilutions. Each symbol represents a single mouse. The overall *P* value for the ANOVA is $P < 0.0001$. Pairwise comparisons were analyzed using an unpaired Mann–Whitney test. $^{**}P = 0.0079$. (*D*) Isopycnic sucrose gradient centrifugation of total membranes isolated from untreated or G5132-treated G5132^R-1 and G5132^R-8 cells. Fractions were probed for LirL expression. MsbA and Pal were used to determine IM (fractions 4 and 5) and OM (fraction 9).

detected in G5132^R-1 and G5132^R-8. Sucrose gradient fractionations demonstrated that G5132^R-1 and G5132^R-8 LirL localized to the IM at levels similar to those seen earlier in wild-type Ab17978 (Fig. 4*D*). In comparison with G5132-treated Ab17978 cells, no further LirL/DG-proLirL accumulation in the IM was detected in G5132-treated G5132^R-1 and G5132^R-8 cells (Fig. 4*D*), suggesting that G5132^R-1 and G5132^R-8 LirL may not be as efficiently processed by LspA.

To address whether the G5132^R mutations lead to less efficient processing by LspA, we introduced the G5132^R-1 mutation into pWH-*lirl*ΔR to generate Ab17978Δ*lirL* expressing his-tagged LirL-ΔR^{G5132R1} and performed mass spectrometry on purified LirL-ΔR and LirL-ΔR^{G5132R1}. The expected molecular weights of triacylated LirL-ΔR and LirL-ΔR^{G5132R1} are expected to be the same (~2.9 kDa) (Fig. 5*A*). Mass spectrometry data confirmed that both wild-type and mutant cells expressed mature triacylated LirL-ΔR to similar levels (Figs. 2*B* and 5*B*). However, unlike that seen in cells expressing LirLΔR, untreated cells expressing LirL-ΔR^{G5132R1} contained additional DG-proLirL-ΔR^{G5132R1} intermediates that were insensitive to G5132 (Fig. 5*B*). These data are consistent with western blot analyses demonstrating that cells expressing LirL-ΔR^{G5132R1} contained G5132-sensitive mature triacylated LirL-ΔR as well as additional G5132-insensitive higher–molecular weight forms of what are expected to be DG-proLirL-ΔR^{G5132R1} (Fig. 5*C*). Interestingly, the LirL-ΔR species profile detected in untreated Ab17978 expressing either *lirL*-ΔR or *lirL*-ΔR^{G5132R1} was similar. These data suggest that unlike that seen with *E. coli* Lpp, the signal peptide mutations in G5132^R cells allow *A. baumannii* to tolerate IM levels of DG-proLirL forms that are not as sensitive to cleavage by LspA and hence, lead to G5132 resistance.

Discussion

Compared with *E. coli*, lipoprotein biosynthesis in *A. baumannii* has been relatively uncharacterized. Although *lspA* is essential for *A. baumannii* growth, the lack of potent LspA inhibitors has prevented a thorough understanding of the resistance mechanisms to these inhibitors. In this study, we identify a potent globomycin analog, G5132, and demonstrate that resistance to G5132 maps to a previously uncharacterized lipoprotein *lirL*, which plays a crucial role in *A. baumannii* cell morphology, serum sensitivity, and virulence.

While resistance to globomycin or its analogs is known to be mediated by deletion or decreased expression of *lpp* (32), mechanisms leading to resistance to LspA inhibitors in *A. baumannii* have remained largely unknown until now. Our data demonstrate that G5132 resistance in three independent *A. baumannii* strains (Ab17978, Ab19606, and AB5075) maps to a previously uncharacterized gene that we confirm encodes a bona fide lipoprotein. Sequence analyses identified *lirL* in all *A. baumannii* isolates and in certain *Pseudomonales*, *Serratia*, and *Parabulkhoderia* species (*SI Appendix*, Fig. S2). In gram-negative bacterial lipoproteins, the +2 amino acid of the mature lipoprotein plays a critical role in localization to the IM or OM (51, 52). While Asp at +2 functions as an IM lipoprotein retention signal in *E. coli*, other positions at +3 and +4 (histidine or lysine) can also be important for lipoprotein sorting (51). The +2 position in

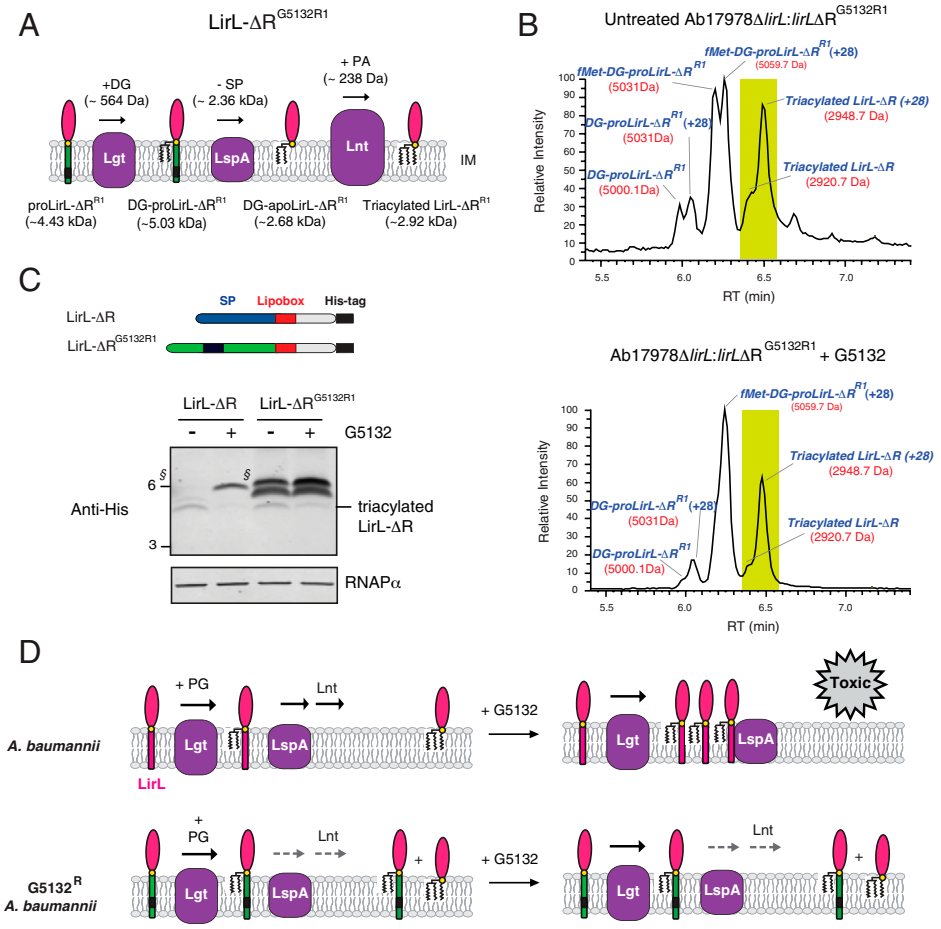

Fig. 5. Signal peptide mutations lead to the accumulation of DG-proLirL in untreated G5132^R cells. (*A*) Predicted molecular weights of LirL-ΔR truncated protein containing G5132^R-1 mutations in the signal peptide (LirL-ΔR^{G5132R1}). PA, palmitic acid; SP, signal peptide. (*B*) LC-UV-MS analysis of purified LirL-ΔR^{G5132R1} from untreated cells or cells treated with 44.4 μg/mL G5132 leads to the accumulation of DG-proLirLΔR^{G5132R1} with or without an N-terminal *fMet* in untreated cells expressing LirL-ΔR^{G5132R1}. As with LirL-ΔR, the +28-Da peak represents LirL-ΔR^{G5132R1} modified with acyl tails containing two additional carbons (CH_2-CH_2). RT denotes retention time. (*C*) Total cell lysates from untreated (−) or G5132-treated (+) Ab17978 expressing His-tagged LirL-ΔR or LirL-ΔR^{G5132R1} were subjected to western blot analysis. RNAPα was used as a loading control ("§" represents DG-proLirL-ΔR, and mature triacylated LirL-ΔR is depicted). (*D*) Proposed model explaining the mechanism of LirL resistance to G5132 in *A. baumannii*. In wild-type *A. baumannii*, LirL is processed by the lipoprotein biosynthetic enzymes Lgt, LspA, and Lnt into triacylated mature LirL localized to the IM. Treatment with G5132 leads to the accumulation of DG-proLirL in the IM, leading to a block in the pathway causing cell death. The G5132^R mutations in the LirL signal peptide lead to DG-proLirL mutants that are not efficiently catalyzed by LspA, which overcomes the obstruction of lipoprotein biosynthetic flux causing G5132 resistance.

LirL is an Ser, suggesting it would localize to the OM, but our data show that LirL is primarily localized to the IM, contradicting the known Lol sorting rules from *E. coli*. Other residues also play a role in determining membrane localization of lipoproteins as demonstrated by Narita and Tokuda (53). Given that LirL contains an Lys at the +3 position, additional studies are warranted to elucidate the amino acid determinants of LirL localization in *A. baumannii*. Unlike with *E. coli*, separation of *A. baumannii* IM and OM is known to be more challenging due, in part, to a unique cell envelope containing LOS (54–56). For this reason, it is unclear if the detection of minor levels of LirL in the OM fractions in our studies also represents an OM localized form or whether this is due to contamination from incomplete membrane separation. Interestingly, a small fraction of proPal can be detected in the OM after G5132 treatment (Figs. 2*H* and 4*D*), which currently cannot be fully explained. Another unexpected finding is that full-length LirL and the truncated LirL-ΔR migrate on SDS-PAGE higher than their predicted molecular weights (Fig. 2). While mass spectrometry of the truncated LirL-ΔR mutant confirms that it has the expected monomeric mass of 2.92 kDa, the full-length LirL contains multiple species that are larger than the theoretical expected molecular weight of triacylated LirL. Although our data suggest that the majority of LirL is not covalently linked to PGN, we cannot rule out the possibility that LirL noncovalently interacts with PGN. Additional studies are needed to determine the identity of the LirL covalent linkages. Polyalanine expansions can lead to protein misfolding and aggregation (57), and the alanine-rich glycosylphosphatidylinositol-linked protein BARP in *Trypanosoma brucei* migrates higher than expected in western blot analyses (58). Cumulatively, our data suggest that LirL is a unique lipoprotein compared with previously identified bacterial lipoproteins, and our study highlights additional questions regarding the role of LirL in *A. baumannii* physiology.

While our data demonstrate that LirL plays a key role in resistance to inhibitors of LspA and that *lirL* deficiency leads to significant defects on OM integrity, cellular morphology, and virulence, the molecular function of LirL in *A. baumannii* still remains unclear. Although complementation of an *lpp*-deleted *E. coli* by either *lirL* or *lpp* rescues resistance to globomycin, our data clearly show that Lpp and LirL do not perform the same functions. Unlike Lpp, LirL is localized to the IM, contains a C-terminal histidine, is not PGN linked, and does not functionally rescue serum sensitivity of an *lpp*-deleted *E. coli* strain. Alanine-rich clusters can form α-helix coiled-coil conformations (59), and alanine-rich proteins have been demonstrated to regulate protein localization (60, 61). It is possible that LirL may serve as a rigid scaffold to provide both structural integrity and enhance protein–protein interactions needed for cell division. Given that *A. baumannii* can adapt to grow in vitro in the absence of *lirL*, additional proteomic and transcriptomic profiling of *lirL*-deleted cells may uncover compensatory mechanisms allowing for bacterial growth in the absence of LirL.

Although deletion of *lirL* leads to resistance to G5132, the mechanism by which mutations in the LirL signal peptide lead to G5132 resistance remains unclear, especially given that G5132^R and wild-type *A. baumannii* strains express similar levels of the triacylated LirL protein. The LirL species detected in G5132^R strains by western blot analyses (Fig. 4*B*) are consistent with our mass spectrometry data (Fig. 5*B*), suggesting that these lower–molecular weight species represent mutant signal

peptide-containing LirL intermediates. Although we do not have direct evidence that DG-proLirL accumulation is toxic in *A. baumannii*, our data suggest that IM accumulation of DG-proLirL may contribute to cell death. Even though LirL is not PGN linked, it is conceivable to hypothesize that G5132 treatment leads to IM accumulation of DG-proLirL, which could prevent efficient flux through the biosynthetic pathway causing cell death (Fig. 5*D*). Although this is supported by our preliminary calculations that LirL is a highly abundant lipoprotein in Ab17978 (*SI Appendix*, Fig. S4*B*), our calculations do have some limitations. First, the unresolved mass of the full-length LirL, aberrant SDS-PAGE migration, and multiple LirL species may affect the predicted number of LirL molecules per CFU. Second, our analyses were performed using Ab17978 and may not reflect the expression of LirL in other pathogenic *A. baumannii* isolates. Further characterization is needed to more accurately determine the abundance of LirL in *A. baumannii*. However, it remains intriguing to speculate that the mutations in G5132^{R} strains could change the signal peptide register in the membrane such that it is less efficiently processed by LspA, resulting in the release of the block in the biosynthetic pathway (Fig. 5*D*). It is worth noting that mutations within mature Lpp (32) or LirL (*SI Appendix*, Table S3) that confer resistance to LspA inhibitors are rarely detected. In summary, our study identifies a highly abundant lipoprotein that confers resistance to LspA inhibitors in *A. baumannii*. Further investigation to elucidate the cellular role of LirL, LirL-interacting proteins, and transcriptional changes in *lirL*-deleted cells will undoubtedly uncover deeper insights into the function of LirL in *A. baumannii*.

Materials and Methods

Ethics Statement. All mice used in this study were housed and maintained at Genentech in accordance with the American Association of Laboratory Animal Care guidelines. All experimental studies were conducted under protocol 19-1290, and they were approved by the Institutional Animal Care and Use Committee of Genentech Lab Animal Research and performed in an Association for Assessment and Accreditation of Laboratory Animal Care International–accredited facility in accordance with the *Guide for the Care and Use of Laboratory Animals* (62) and applicable laws and regulations.

Bacterial Strains and Plasmids. The *A. baumannii* strains (Ab19606, Ab17978) and the *E. coli* strain CFT073 (ATCC 700928) were purchased from ATCC. The *A. baumannii* AB5075-UW Mutant Library and the wild-type parental strain AB5075-UW were obtained from the Manoil laboratory at the University of Washington, Seattle. Clinical *A. baumannii* isolates were obtained from the IHMA or the CDC. Methicillin-resistant *S. aureus* strain USA300 was also used in this study. Detailed methods for the generation of additional bacterial strains are provided in *SI Appendix*. All bacterial strains and primers used in this study are listed in *SI Appendix*, Tables S6 and S7, respectively.

SDS-PAGE and Western Blot Analyses. Western blot analysis was performed as described previously (32), with some modifications. Bacterial cells were resuspended and lysed in BugBuster Protein Extraction Reagent containing 20 U/mL benzonase and 1,000 U/mL lysonase (Novagen). Cell lysates were mixed with equivalent volume of 2× SDS sample buffer (LI-COR 928-40004 containing 5% 2-mercaptoethanol) and heated at 95 °C for 15 min before loading. Detailed methods are provided in *SI Appendix*.

Expression and Purification of Recombinant LirL. Residues Ser_{22}-His_{83} of *A. baumannii* LirL were cloned into a modified pAcGP67A vector downstream of the polyhedron promoter containing an N-terminal His6-tag and a C-terminal Flag-tag (His_6-LirL-Flag). Recombinant baculovirus was generated using the Baculogold system (BD Biosciences) following standard protocols. Detailed methods are provided in *SI Appendix*.

In Vitro Bacterial Growth, Frequency of Resistance, OMV Quantitation and Serum Resistance Assays, and Mammalian Cell Culture. Bacterial cultures were started by inoculating a single bacterial colony from Tryptic soy agar plates into Tryptic soy broth, and the cultures were grown overnight at 37 °C. FOR (32) and serum resistance experiments (48) were performed as previously described for *E. coli*, with some modifications. To determine the role of the second nonessential annotated type II signal peptidase gene, we compared FOR of the parental strains with their corresponding mutants (Ab19606Δ*DJ41_RS04640* and AB09365). For *K. pneumoniae* 700603, Ab19606Δ*DJ41_RS04640*, and AB09365, we tested three independent overnight cultures due to compound limitations. For all other strains, 10 independent overnight cultures were tested. Quantitation of OMV as well as culture of Raw264.7 macrophages and their infection to measure bacterial clearance were performed as previously described (63).

Mass Spectrometry of Purified LirL-ΔR and LirL-ΔR^{G5132R1}. Liquid chromatography UV mass spectrometry (LC-UV-MS) analyses were performed as described previously (64).

Mouse Infection Model. To determine the role of LirL in vivo, we tested Ab17978Δ*lirL*, Ab17978-G1532^{R} mutants 1 and 8 (G1532^{R}-1 and G1532^{R}-8), and Ab17978Δ*lnt* virulence in a neutropenic lung infection model. CFU was enumerated in the lung homogenates through serial dilutions at 2 and 24 h postinfection. Additional details are provided in *SI Appendix*.

Transmission Electron, Time-Lapse, and Confocal Microcopy. Transmission electron microscopy, time-lapse microcopy, and confocal microcopy were performed as described previously (64). Details are provided in *SI Appendix*.

Isopycnic Sucrose Gradient Centrifugation. Sucrose gradient fractionation of the *A. baumannii* membranes was performed with freshly prepared bacteria pellets based on the protocol described by Cian et al. (54), with some modifications.

Ab17978, Ab17978_G5132^{R}-1, and Ab17978_G5132^{R}-8 strains were transformed with pWH-*pal*, grown to approximately optical density $(OD)_{600} = 0.8$, and left untreated (0.5% dimethyl sulfoxide) or treated with 44.4 μg/mL G5132 for 1 h. The bacteria pellets were harvested, and membrane proteins were fractionated through a sucrose gradient composed of 1.5 mL of 20% sucrose, 6 mL of 45% sucrose, and 3 mL of 73% sucrose (from top to bottom). Fractions of 1 mL were collected from the top to the bottom for western blot analyses.

Purification of PAPs. Purification of PAPs was performed according to published methods (44, 45) with some modifications. After PAP extraction, the sample was subjected to centrifugation at 100,000 × *g* for 60 min at 22 °C; the pellet containing PGN and associated proteins was washed once, subjected to centrifugation at 100,000 × *g* for 30 min, and resuspended in PAP extraction buffer (referred to as the SDS insoluble on PAP fraction). The supernatant containing the SDS-soluble fraction was aliquoted and frozen (referred to as the non-PAP fraction).

Statistical Analyses. All statistical analyses were performed using GraphPad Prism 6.0 software (GraphPad). The data were tested for being parametric, and statistical analyses were performed on log-transformed data. All graphs represent the mean ± SEM. Unless stated otherwise, *P* values for all data were determined using the Mann–Whitney unpaired *t* test (*$P < 0.05$, **$P < 0.01$, and ***$P < 0.001$).

WGS and Variant Detection. WGS and variant analysis were performed as previously described (32). Ab17879 (accession nos. NZ_CP012004.1 and NZ_CP012005.1) and Ab19606 (GenBank accession nos. NZ_KL810966.1 and NZ_KL810967.1) reference genomes were used for variant detection. The sequences reported in this paper have been deposited in the NCBI Sequence Read Archive (accession nos. SAMN30006377–SAMN30006414 [BioProject PRJNA863033]).

Data, Materials, and Software Availability. The DNA sequence has been deposited in the National Center for Biotechnology Information Sequence Read Archive (accession nos. SAMN30006377– SAMN30006414 [BioProject PRJNA863033]) (65). All other data are included in the article and/or *SI Appendix*.

ACKNOWLEDGMENTS. This study was supported by internal Genentech funds. The funders had no role in study design, data collection and analysis, decision to publish, or preparation of the manuscript. We thank Kelly Storek for her feedback on the manuscript and Hany Girgis for pATO2. We also thank Georgette Castanedo; Keira and Paul Gibbons for help with the synthesis of G5132; Jian Payandeh, Jawahar Sudhamsu, and the BioMolecular Resources group for the expression and purification of recombinant LirL protein; and Scott Stawicki for assistance with generating the rabbit polyclonal antibodies.

Author affiliations: [a]Department of Infectious Diseases, Genentech, South San Francisco, CA 94080; [b]Department of Ophthalmology, Metabolism, Neuroscience, Immunology and Infectious Diseases Bioinformatics, Genentech, South San Francisco, CA 94080; [c]Department of Microchemistry, Proteomics and Lipidomics, Genentech, South San Francisco, CA 94080; [d]Department of Pathology, Genentech, South San Francisco, CA 94080; [e]Department of Translational Immunology, Genentech, South San Francisco, CA 94080; [f]Department of Structural Biology, Genentech, South San Francisco, CA 94080; and [g]Department of Chemistry, Genentech, South San Francisco, CA 94080

Author contributions: K.-J.H., M.-W.T., and S.B.K. designed research; K.-J.H., H.P., J.D., M.V., W.S., V.T., Y.P., M.S., D.Y., J.K., A.K.K., N.M., and M.R. performed research; E.S. and E.H. contributed new reagents/analytic tools; K.-J.H., H.P., J.D., E.S., M.V., W.S., V.T., Y.P., M.S., D.Y., J.K., A.K.K., N.M., M.R., C.D.A., M.X., and S.B.K. analyzed data; M.W.T. contributed key insights; M.X. oversaw in vivo experiments and strategy; S.B.K. oversaw overall research strategy; and K.-J.H. and S.B.K. wrote the paper.

Competing interest statement: This study was supported by internal Genentech funds. All authors are or were employees of Genentech, a member of the Roche Group, and all authors except V.T. are shareholders of Roche.

1. P. E. Fournier, H. Richet, The epidemiology and control of *Acinetobacter baumannii* in health care facilities. *Clin. Infect. Dis.* **42**, 692–699 (2006).
2. C.-R. Lee *et al.*, Biology of *Acinetobacter baumannii*: Pathogenesis, antibiotic resistance mechanisms, and prospective treatment options. *Front. Cell. Infect. Microbiol.* **7**, 55 (2017).
3. N. C. Gordon, D. W. Wareham, Multidrug-resistant *Acinetobacter baumannii*: Mechanisms of virulence and resistance. *Int. J. Antimicrob. Agents* **35**, 219–226 (2010).
4. M.-F. Lin, C.-Y. Lan, Antimicrobial resistance in *Acinetobacter baumannii*: From bench to bedside. *World J. Clin. Cases* **2**, 787–814 (2014).
5. R. Gaynes, J. R. Edwards, N. N. I. S. System; National Nosocomial Infections Surveillance System, Overview of nosocomial infections caused by Gram-negative bacilli. *Clin. Infect. Dis.* **41**, 848–854 (2005).
6. L. K. Logan, S. Gandra, A. Trett, R. A. Weinstein, R. Laxminarayan, *Acinetobacter baumannii* resistance trends in children in the United States, 1999-2012. *J. Pediatric Infect. Dis. Soc.* **8**, 136–142 (2019).
7. M. Tatman-Otkun, S. Gürcan, B. Ozer, N. Shokrylanbaran, Annual trends in antibiotic resistance of nosocomial *Acinetobacter baumannii* strains and the effect of synergistic antibiotic combinations. *New Microbiol.* **27**, 21–28 (2004).
8. T. J. Silhavy, D. Kahne, S. Walker, The bacterial cell envelope. *Cold Spring Harb. Perspect. Biol.* **2**, a000414 (2010).
9. C. Whitfield, M. S. Trent, Biosynthesis and export of bacterial lipopolysaccharides. *Annu. Rev. Biochem.* **83**, 99–128 (2014).
10. J. M. Boll *et al.*, A penicillin-binding protein inhibits selection of colistin-resistant, lipooligosaccharide-deficient *Acinetobacter baumannii*. *Proc. Natl. Acad. Sci. U.S.A.* **113**, E6228–E6237 (2016).
11. C. E. Cowles, Y. Li, M. F. Semmelhack, I. M. Cristea, T. J. Silhavy, The free and bound forms of Lpp occupy distinct subcellular locations in *Escherichia coli*. *Mol. Microbiol.* **79**, 1168–1181 (2011).
12. M. M. Wilson, H. D. Bernstein, Surface-exposed lipoproteins: An emerging secretion phenomenon in Gram-negative bacteria. *Trends Microbiol.* **24**, 198–208 (2015).
13. A. Kovacs-Simon, R. W. Titball, S. L. Michell, Lipoproteins of bacterial pathogens. *Infect. Immun.* **79**, 548–561 (2011).
14. M. J. Schlesinger, *Lipid Modifications of Proteins* (CRC Press, 1992).
15. M. Tokunaga, H. Tokunaga, H. C. Wu, Post-translational modification and processing of *Escherichia coli* prolipoprotein in vitro. *Proc. Natl. Acad. Sci. U.S.A.* **79**, 2255–2259 (1982).
16. S. Olatunji *et al.*, Structures of lipoprotein signal peptidase II from *Staphylococcus aureus* complexed with antibiotics globomycin and myxovirescin. *Nat. Commun.* **11**, 140–11 (2020).
17. I. K. Dev, R. J. Harvey, P. H. Ray, Inhibition of prolipoprotein signal peptidase by globomycin. *J. Biol. Chem.* **260**, 5891–5894 (1985).
18. K. Gerth, H. Irschik, H. Reichenbach, W. Trowitzsch, The myxovirescins, a family of antibiotics from *Myxococcus virescens* (Myxobacterales). *J. Antibiot. (Tokyo)* **35**, 1454–1459 (1982).
19. Y. Xiao, K. Gerth, R. Müller, D. Wall, Myxobacterium-produced antibiotic TA (myxovirescin) inhibits type II signal peptidase. *Antimicrob. Agents Chemother.* **56**, 2014–2021 (2012).
20. C. M. Gwin *et al.*, The apolipoprotein N-acyl transferase Lnt is dispensable for growth in Acinetobacter species. *Microbiology (Reading)* **164**, 1547–1556 (2018).
21. E. D. LoVullo, L. F. Wright, V. Isabella, J. F. Huntley, M. S. Pavelka, Revisiting the Gram-negative lipoprotein paradigm. *J. Bacteriol.* **197**, 1705–1715 (2015).
22. F. C. Neidhardt, "Chemical composition of *Escherichia coli*" in *Escherichia coli and Salmonella: Cellular and Molecular Biology*, F. C. Neidhardt, Ed. (ASM Press, Washington, DC, ed. 2, 1996), pp. 1035–1063.
23. V. Braun, U. Sieglin, The covalent murein-lipoprotein structure of the *Escherichia coli* cell wall. The attachment site of the lipoprotein on the murein. *Eur. J. Biochem.* **13**, 336–346 (1970).
24. V. Braun, H. Wolff, The murein-lipoprotein linkage in the cell wall of *Escherichia coli*. *Eur. J. Biochem.* **14**, 387–391 (1970).
25. Y. Hirota, H. Suzuki, Y. Nishimura, S. Yasuda, On the process of cellular division in *Escherichia coli*: A mutant of *E. coli* lacking a murein-lipoprotein. *Proc. Natl. Acad. Sci. U.S.A.* **74**, 1417–1420 (1977).
26. H. Suzuki *et al.*, Murein-lipoprotein of *Escherichia coli*: A protein involved in the stabilization of bacterial cell envelope. *Mol. Gen. Genet.* **167**, 1–9 (1978).
27. D. W. Yem, H. C. Wu, Physiological characterization of an *Escherichia coli* mutant altered in the structure of murein lipoprotein. *J. Bacteriol.* **133**, 1419–1426 (1978).
28. L. J. Zwiebel, M. Inukai, K. Nakamura, M. Inouye, Preferential selection of deletion mutations of the outer membrane lipoprotein gene of *Escherichia coli* by globomycin. *J. Bacteriol.* **145**, 654–656 (1981).
29. S. M. McLeod, *et al.*, Small molecule inhibitors of gram-negative lipoprotein trafficking discovered by phenotypic screening. *J. Bacteriol.* **197**, 1075–1082 (2015).
30. N. N. Nickerson *et al.*, A novel inhibitor of the LolCDE ABC transporter essential for lipoprotein trafficking in Gram-negative bacteria. *Antimicrob. Agents Chemother.* **62**, e02151-17 (2018).
31. T. Yakushi, T. Tajima, S. Matsuyama, H. Tokuda, Lethality of the covalent linkage between mislocalized major outer membrane lipoprotein and the peptidoglycan of *Escherichia coli*. *J. Bacteriol.* **179**, 2857–2862 (1997).
32. H. Pantua, *et al.*, Unstable mechanisms of resistance to inhibitors of *Escherichia coli* lipoprotein signal peptidase. *mBio* **11**, e02018–e02020 (2020).
33. K. Garland *et al.*, Optimization of globomycin analogs as novel Gram-negative antibiotics. *Bioorg. Med. Chem. Lett.* **30**, 127419 (2020).
34. M. F. Richter *et al.*, Predictive compound accumulation rules yield a broad-spectrum antibiotic. *Nature* **545**, 299–304 (2017).
35. N. Buddelmeijer, The molecular mechanism of bacterial lipoprotein modification–how, when and why? *FEMS Microbiol. Rev.* **39**, 246–261 (2015).
36. M. T. Nguyen, F. Götz, Lipoproteins of gram-positive bacteria: Key players in the immune response and virulence. *Microbiol. Mol. Biol. Rev.* **80**, 891–903 (2016).
37. B. A. Evans, S. G. B. Amyes, OXA β-lactamases. *Clin. Microbiol. Rev.* **27**, 241–263 (2014).
38. L. A. Gallagher *et al.*, Resources for genetic and genomic analysis of emerging pathogen *Acinetobacter baumannii*. *J. Bacteriol.* **197**, 2027–2035 (2015).
39. J. El Rayes, R. Rodríguez-Alonso, J.-F. Collet, Lipoproteins in Gram-negative bacteria: New insights into their biogenesis, subcellular targeting and functional roles. *Curr. Opin. Microbiol.* **61**, 25–34 (2021).
40. M. M. Babu *et al.*, A database of bacterial lipoproteins (DOLOP) with functional assignments to predicted lipoproteins. *J. Bacteriol.* **188**, 2761–2773 (2006).
41. A. Albrecht, S. Mundlos, The other trinucleotide repeat: Polyalanine expansion disorders. *Curr. Opin. Genet. Dev.* **15**, 285–293 (2005).
42. G. L. Holliday, J. D. Fischer, J. B. O. Mitchell, J. M. Thornton, Characterizing the complexity of enzymes on the basis of their mechanisms and structures with a bio-computational analysis. *FEBS J.* **278**, 3835–3845 (2011).
43. J. Bravo *et al.*, Identification of a novel bond between a histidine and the essential tyrosine in catalase HPII of *Escherichia coli*. *Protein Sci.* **6**, 1016–1023 (1997).
44. T. Nakae, J. Ishii, M. Tokunaga, Subunit structure of functional porin oligomers that form permeability channels in the other membrane of *Escherichia coli*. *J. Biol. Chem.* **254**, 1457–1461 (1979).
45. C. Whitfield, R. E. Hancock, J. W. Costerton, Outer membrane protein K of *Escherichia coli*: Purification and pore-forming properties in lipid bilayer membranes. *J. Bacteriol.* **156**, 873–879 (1983).
46. H. Nikaido, Outer membrane barrier as a mechanism of antimicrobial resistance. *Antimicrob. Agents Chemother.* **33**, 1831–1836 (1989).
47. M.-D. Phan *et al.*, The serum resistome of a globally disseminated multidrug resistant uropathogenic *Escherichia coli* clone. *PLoS Genet.* **9**, e1003834 (2013).
48. J. Diao *et al.*, Peptidoglycan association of murein lipoprotein is required for KpsD-dependent group 2 capsular polysaccharide expression and serum resistance in a uropathogenic *Escherichia coli* isolate. *mBio* **8**, e00603–e00617 (2017).
49. C. Schwechheimer, M. J. Kuehn, Outer-membrane vesicles from Gram-negative bacteria: Biogenesis and functions. *Nat. Rev. Microbiol.* **13**, 605–619 (2015).
50. N. Lee, H. Yamagata, M. Inouye, Inhibition of secretion of a mutant lipoprotein across the cytoplasmic membrane by the wild-type lipoprotein of the *Escherichia coli* outer membrane. *J. Bacteriol.* **155**, 407–411 (1983).
51. K. Yamaguchi, F. Yu, M. Inouye, A single amino acid determinant of the membrane localization of lipoproteins in *E. coli*. *Cell* **53**, 423–432 (1988).
52. M. Terada, T. Kuroda, S. I. Matsuyama, H. Tokuda, Lipoprotein sorting signals evaluated as the LolA-dependent release of lipoproteins from the cytoplasmic membrane of *Escherichia coli*. *J. Biol. Chem.* **276**, 47690–47694 (2001).
53. S. Narita, H. Tokuda, Amino acids at positions 3 and 4 determine the membrane specificity of *Pseudomonas aeruginosa* lipoproteins. *J. Biol. Chem.* **282**, 13372–13378 (2007).
54. M. B. Cian, N. P. Giordano, J. A. Mettlach, K. E. Minor, Z. D. Dalebroux, Separation of the cell envelope for Gram-negative bacteria into inner and outer membrane fractions with technical adjustments for *Acinetobacter baumannii*. *J. Vis. Exp.*, 10.3791/60517 (2020).
55. K. J. I. Thorne, M. J. Thornley, A. M. Glauert, Chemical analysis of the outer membrane and other layers of the cell envelope of *Acinetobacter* sp. *J. Bacteriol.* **116**, 410–417 (1973).
56. E. Geisinger, W. Huo, J. Hernandez-Bird, R. R. Isberg, *Acinetobacter baumannii*: Envelope determinants that control drug resistance, virulence, and surface variability. *Annu. Rev. Microbiol.* **73**, 481–506 (2019).
57. J. Amiel, D. Trochet, M. Clément-Ziza, A. Munnich, S. Lyonnet, Polyalanine expansions in human. *Hum. Mol. Genet.* **13**, R235–R243 (2004).
58. D. P. Nolan *et al.*, Characterization of a novel alanine-rich protein located in surface microdomains in *Trypanosoma brucei*. *J. Biol. Chem.* **275**, 4072–4080 (2000).
59. R. J. LaPolla *et al.*, Sequence and structural analysis of surface protein antigen I/II (SpaA) of Streptococcus sobrinus. *Infect. Immun.* **59**, 2677–2685 (1991).
60. R. G. Holt, L. Raju, Signal sequence and alanine-rich region of streptococcal protein antigen A of *Streptococcus sobrinus* can direct localization of alkaline phosphatase to the periplasm of *Escherichia coli*. *FEMS Microbiol. Lett.* **184**, 17–21 (2000).
61. S.-H. Chang, W.-L. Chang, C.-C. Lu, W.-Y. Tarn, Alanine repeats influence protein localization in splicing speckles and paraspeckles. *Nucleic Acids Res.* **42**, 13788–13798 (2014).
62. National Research Council, *Guide for the Care and Use of Laboratory Animals* (National Academies Press, Washington, DC, ed. 8, 2011).
63. V. Tiku *et al.*, Outer membrane vesicles containing OmpA induce mitochondrial fragmentation to promote pathogenesis of *Acinetobacter baumannii*. *Sci. Rep.* **11**, 618 (2021).
64. J. Diao *et al.*, Inhibition of *Escherichia coli* lipoprotein diacylglyceryl transferase is insensitive to resistance caused by deletion of Braun's lipoprotein. *J. Bacteriol.* **203**, e0014921 (2021).
65. K. Huang, E. Skippington, S. B. Kapadia, G5132 resistant Acinetobacter baumannii. National Center for Biotechnology Information Sequence Read Archive. https://www.ncbi.nlm.nih.gov/bioproject/PRJNA863033. Deposited 27 July 2022.